

## [Regular Paper]

# Estimation of Gas Composition and Cage Occupancies in CH<sub>4</sub>-C<sub>2</sub>H<sub>6</sub> Hydrates by CP-MAS <sup>13</sup>C NMR Technique

Masato KIDA <sup>†1)</sup>, Hirotohi SAKAGAMI <sup>†1)</sup>, Nobuo TAKAHASHI <sup>†1)\*</sup>, Akihiro HACHIKUBO <sup>†2)</sup>, Hitoshi SHOJI <sup>†2)</sup>, Yasushi KAMATA <sup>†3),†5)</sup>, Takao EBINUMA <sup>†3)</sup>, Hideo NARITA <sup>†3)</sup>, and Satoshi TAKEYA <sup>†4)</sup>

<sup>†1)</sup> Dept. of Materials Science, Kitami Institute of Technology, 165 Koen-cho, Kitami, Hokkaido 090-8507, JAPAN

<sup>†2)</sup> New Energy Resources Research Center, Kitami Institute of Technology, 165 Koen-cho, Kitami, Hokkaido 090-8507, JAPAN

<sup>†3)</sup> Methane Hydrate Research Laboratory, National Institute of Advanced Industrial Science and Technology (AIST), 2-17 Tukisamu-Higashi, Toyohira-ku, Sapporo 062-8517, JAPAN

<sup>†4)</sup> Research Institute of Instrumentation Frontier, National Institute of Advanced Industrial Science and Technology (AIST), Central 5, 1-1-1 Higashi, Tsukuba, Ibaraki 305-8565, JAPAN

(Received August 25, 2006)

CP-MAS <sup>13</sup>C NMR measurements were carried out on mixed gas hydrates containing CH<sub>4</sub>-C<sub>2</sub>H<sub>6</sub>. The changes in NMR chemical shift values for CH<sub>4</sub> and C<sub>2</sub>H<sub>6</sub> clearly corresponded to the structural changes in the hydrate structure. The encaged gas compositions estimated by the integrated <sup>13</sup>C NMR signal intensities agreed well with the dissociated gas compositions measured by gas chromatography. Therefore, the gas composition in mixed gas hydrates can be directly estimated from the <sup>13</sup>C NMR spectra. The cage occupancies of the small and large cages of the hydrates were estimated from the <sup>13</sup>C NMR spectra on the basis of a statistical thermodynamic model. The large cages were almost fully occupied with guest molecules, whereas small cage occupancy decreased with increasing C<sub>2</sub>H<sub>6</sub> concentration. Therefore, large cages are highly preferentially occupied by C<sub>2</sub>H<sub>6</sub> molecules rather than CH<sub>4</sub> molecules.

## Keywords

Gas hydrate, Natural gas, Gas composition, Cage occupancy, <sup>13</sup>C NMR

## 1. Introduction

Natural gas hydrates are expected to provide natural gas resources in the future. The scientific fundamentals and the technical developments relevant to gas hydrates were recently reviewed<sup>1)</sup>. Gas hydrates are crystalline clathrate compounds which are stable under low-temperature and high-pressure conditions. The cages of natural gas hydrates mainly contain methane (CH<sub>4</sub>). However, other hydrocarbons such as ethane (C<sub>2</sub>H<sub>6</sub>), propane (C<sub>3</sub>H<sub>8</sub>), and isobutane (*i*-C<sub>4</sub>H<sub>10</sub>) may be encaged together with CH<sub>4</sub><sup>2)</sup>. Three crystallographic structures are known for gas hydrates, structure I (sI), structure II (sII), and structure H (sH)<sup>1),3)</sup>. Both C<sub>2</sub>H<sub>6</sub> hydrate and CH<sub>4</sub> hydrate have the sI structure, in which the unit cell consists of 46 H<sub>2</sub>O molecules (two small cages with twelve pentagonal faces (5<sup>12</sup>), and six large cages with twelve pentagonal and two hexagonal faces

(5<sup>12</sup>6<sup>2</sup>)). Mixed gas hydrates containing CH<sub>4</sub>-C<sub>2</sub>H<sub>6</sub> with appropriate gas compositions have the sII structure, in which the unit cell consists of 136 H<sub>2</sub>O molecules (sixteen small cages with twelve pentagonal faces (5<sup>12</sup>) and eight large cages with twelve pentagonal and four hexagonal faces (5<sup>12</sup>6<sup>4</sup>))<sup>4)</sup>.

The structure of natural gas hydrates is important to clarify for the estimation of the amount of natural gas, since the gas capacity in the hydrate crystal depends on the structure. The X-ray diffraction (XRD) method has been widely used to determine gas hydrate structures<sup>2),3),5)</sup>. <sup>13</sup>C NMR spectroscopy is also useful to determine hydrate structures containing hydrocarbons<sup>2),4),6)</sup>.

The cage occupancy is defined as the ratio of (number of cages occupied by guest molecules)/(number of total cages), and is also important to estimate the amount of natural gas, since it depends on the conditions of the hydrate formation such as pressure and gas composition. In general, samples of synthesized gas hydrates and natural gas hydrates recovered from sea floor contain a certain amount of frozen water<sup>5),7)</sup>. Therefore, the cage occupancy is difficult to estimate from the amounts of water and gas obtained by dissociation of

\* To whom correspondence should be addressed.

\* E-mail: takanb@mail.kitami-it.ac.jp

<sup>†5)</sup>(Present) Disaster Prevention Technology Div., Railway Technical Research Institute, 2-8-38 Hikari-cho, Kokubunji, Tokyo 185-8540, JAPAN

the sample. Raman spectroscopy has been used to estimate the cage occupancy in the case of the CH<sub>4</sub>-C<sub>2</sub>H<sub>6</sub> mixed system<sup>4,8</sup>), in which the values for the cage occupancies were calculated without considering the effect of the frozen water. However, Raman spectroscopy cannot easily distinguish the signals of CH<sub>4</sub> from those of other heavier hydrocarbons such as C<sub>3</sub>H<sub>8</sub><sup>9</sup>). Therefore, the establishment of techniques other than Raman spectroscopy is important to estimate the cage occupancies in natural gas hydrates.

<sup>13</sup>C NMR (nuclear magnetic resonance) of sII natural gas hydrate containing hydrocarbons such as CH<sub>4</sub>, C<sub>2</sub>H<sub>6</sub>, C<sub>3</sub>H<sub>8</sub>, and *i*-C<sub>4</sub>H<sub>10</sub> was found to distinguish the hydrocarbon molecules in different cages<sup>2</sup>). Therefore, the cage occupancies could be estimated from the <sup>13</sup>C NMR data on the basis of the statistical thermodynamic model<sup>6,10</sup>). Additionally, the <sup>13</sup>C NMR technique can be applied to more complex gas systems<sup>11</sup>). Thus, the <sup>13</sup>C NMR technique may be effective for the determination of crystal structure and for the estimation of cage occupancies. However, suitable high quality spectra are difficult to obtain for natural gas hydrate samples because of the low natural abundance of <sup>13</sup>C and the low concentration of natural gas hydrate in the samples recovered from the sea floor<sup>7</sup>). Therefore, the <sup>13</sup>C NMR measurement technique must be improved for the analysis of natural gas hydrate samples. The solid-state <sup>13</sup>C NMR method using the Cross Polarization and Magic Angle Spinning (CP-MAS) technique can effectively enhance the signal intensities<sup>4,6,12,13</sup>). In addition, such enhancement in signal intensities is possible at lower temperatures, in contrast to previous <sup>13</sup>C NMR measurements of the hydrate samples which were usually carried out at 193-253 K<sup>4,6</sup>).

In the present study, CP-MAS <sup>13</sup>C NMR analyses of the mixed CH<sub>4</sub>-C<sub>2</sub>H<sub>6</sub> gas hydrate system were carried out at 163 K, and the cage occupancies of the guest molecules in mixed gas hydrates containing CH<sub>4</sub> and C<sub>2</sub>H<sub>6</sub> were estimated.

## 2. Experimental

Pure CH<sub>4</sub> and C<sub>2</sub>H<sub>6</sub> hydrates were prepared from ice particles and the corresponding hydrocarbon gases using a milling-type high-pressure vessel. Mixed CH<sub>4</sub>-C<sub>2</sub>H<sub>6</sub> gas hydrates were prepared in the same way using gas mixtures with the desired compositions. The preparation method was as follows. Small (0.5-1.0 mm) ice particles (30 g) were loaded into the high-pressure vessel (1 × 10<sup>-3</sup> m<sup>3</sup>) with two stainless steel rods for mixing, and the gas (1.5-1.8 MPa) was introduced into the vessel (gas composition analyzed by gas chromatography). The ice particles were milled by the stainless steel rods in the rotating vessel (*ca.* 50 rpm) in a cold room at 263 K. A decrease in pressure of 0.1-0.3 MPa was observed as a result of hydrate

formation. The hydrate samples were recovered from the vessel at liquid N<sub>2</sub> temperature. A small portion of the sample was decomposed in a small vessel to analyze the dissociated gases by gas chromatography.

The <sup>13</sup>C NMR spectra of the hydrate samples were measured by an NMR spectrometer (JEOL model JNM-AL400, 100 MHz) equipped with a probe for solid samples (JEOL model SH40T6) at 163 K using cooled dry N<sub>2</sub> gas. Almost no appreciable decreases in the signal intensities were observed during the measurements at 163 K. The hydrate samples were introduced into a zirconia sample tube (JEOL; diameter: 6 mm, length: 22 mm) in liquid N<sub>2</sub>. CP-MAS <sup>13</sup>C NMR measurement of hydrocarbon hydrates requires long contact time for the quantitative analysis<sup>6</sup>). Therefore, the CP-MAS <sup>13</sup>C NMR measurements were carried out under the following conditions: contact time 10 ms, pulse delay time 50 s, number of acquisitions 40-400 (depending on the S/N ratio), and spinning rate 3.0-4.0 kHz at the magic angle. The values of the <sup>13</sup>C chemical shift were determined using adamantane as an external reference material with the methyl carbon peak at 298 K set at 29.472 ppm<sup>14</sup>). <sup>13</sup>C single-pulse NMR measurements were carried out under the following conditions: <sup>13</sup>C pulse length 5.5 μs (90°), pulse delay time 50 s for complete relaxation of the samples, number of acquisitions 80 and 200 (depending on the S/N ratio), and spinning rate 3.8 kHz at the magic angle.

## 3. Results and Discussion

CP-MAS <sup>13</sup>C NMR spectra of pure CH<sub>4</sub> and pure C<sub>2</sub>H<sub>6</sub> hydrates are shown in **Fig. 1 (a)** and **(e)**, respectively. The CH<sub>4</sub> hydrate was characterized by two peaks at chemical shifts of -4.14 ppm and -6.52 ppm, attributed to CH<sub>4</sub> molecules in the small and large cages of sI, respectively. The C<sub>2</sub>H<sub>6</sub> hydrate was characterized by a single peak at 7.95 ppm, assigned to C<sub>2</sub>H<sub>6</sub> molecules in the large cage of sI (5<sup>12</sup>6<sup>2</sup>), since C<sub>2</sub>H<sub>6</sub> is too large for the small cage (5<sup>12</sup>). The present peaks correspond to those already reported<sup>4</sup>).

In the mixed gas hydrates containing CH<sub>4</sub> and C<sub>2</sub>H<sub>6</sub>, the concentration of C<sub>2</sub>H<sub>6</sub> in the hydrate phase (determined by gas chromatography and denoted as  $y_E^{GC}$ ) was different from that in the initial feed mixed gas (denoted as  $x_E$ ). For example, the mixed gas with  $x_E = 1.1\%$  yielded a hydrate with  $y_E^{GC} = 18\%$ . The relationship between  $x_E$  and  $y_E^{GC}$  has been reported elsewhere<sup>4,8</sup>). Typical CP-MAS <sup>13</sup>C NMR spectra of the mixed gas hydrates are also shown in **Fig. 1**. The crystallographic structure of the mixed gas hydrate with  $y_E^{GC} = 18\%$  is sII<sup>8</sup>). The spectrum **(b)** of this sample included three NMR peaks at 6.50 ppm, -4.04 ppm, and -7.88 ppm, which were attributed to C<sub>2</sub>H<sub>6</sub> in 5<sup>12</sup>6<sup>4</sup>, CH<sub>4</sub> in 5<sup>12</sup>, and CH<sub>4</sub> in 5<sup>12</sup>6<sup>4</sup>, respectively, on the basis of the previous study<sup>4</sup>). Spectrum **(c)** of the sample with

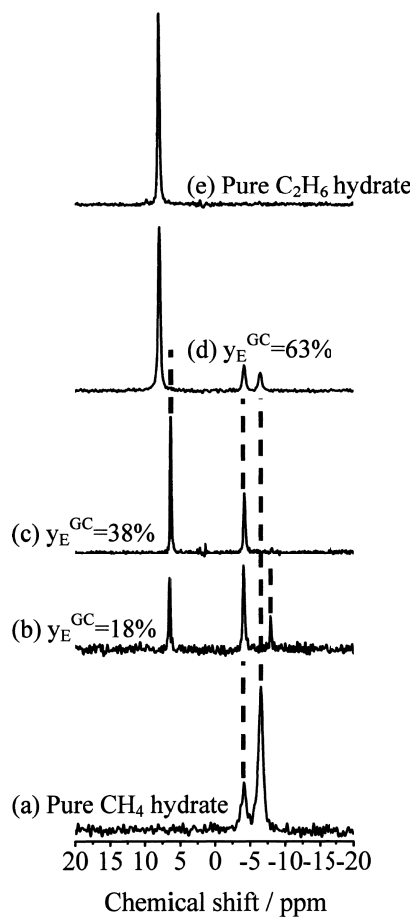


Fig. 1 CP-MAS  $^{13}\text{C}$  NMR Spectra of Pure  $\text{CH}_4$  Hydrate, Pure  $\text{C}_2\text{H}_6$  Hydrate, and Mixed  $\text{CH}_4$ - $\text{C}_2\text{H}_6$  Hydrates at 163 K

$y_E^{\text{GC}} = 38\%$  ( $x_E = 15\%$ ) showed three peaks at the same positions, indicating the **sII** structure. However, the peak intensity of  $\text{CH}_4$  in  $5^{12}6^4$  in spectrum (c) was much smaller than that in spectrum (b). On the other hand, spectrum (d) showed the chemical shifts of the sample with  $y_E^{\text{GC}} = 63\%$  ( $x_E = 30\%$ ) were almost the same as those for pure  $\text{CH}_4$  and  $\text{C}_2\text{H}_6$  hydrates indicating the **sI** structure. In the present study, CP-MAS  $^{13}\text{C}$  NMR measurements were carried out on eight samples in the range of  $18 \leq y_E^{\text{GC}} \leq 85\%$ . The observed chemical shifts are shown in Fig. 2. The changes in the chemical shifts for  $\text{CH}_4$  and  $\text{C}_2\text{H}_6$  in the large cages ( $5^{12}6^2$  for **sI** and  $5^{12}6^4$  for **sII**) clearly reflected the crystallographic changes according to the changes in the gas composition of the  $\text{CH}_4$ - $\text{C}_2\text{H}_6$  mixture. The observed structural changes associated with the  $\text{C}_2\text{H}_6$  concentration were consistent with those already reported<sup>(4),5),8)</sup>.

Gas composition can be estimated from the  $^{13}\text{C}$  NMR peak intensities assigned to  $\text{CH}_4$  and  $\text{C}_2\text{H}_6$  in the case of mixed gas hydrates containing  $\text{CH}_4$ - $\text{C}_2\text{H}_6$ , without requiring the Cross Polarization (CP) technique. The concentration of  $\text{C}_2\text{H}_6$  determined by  $^{13}\text{C}$  NMR (denoted by  $y_E^{\text{NMR}}$ ) can be evaluated by Eq. (1).

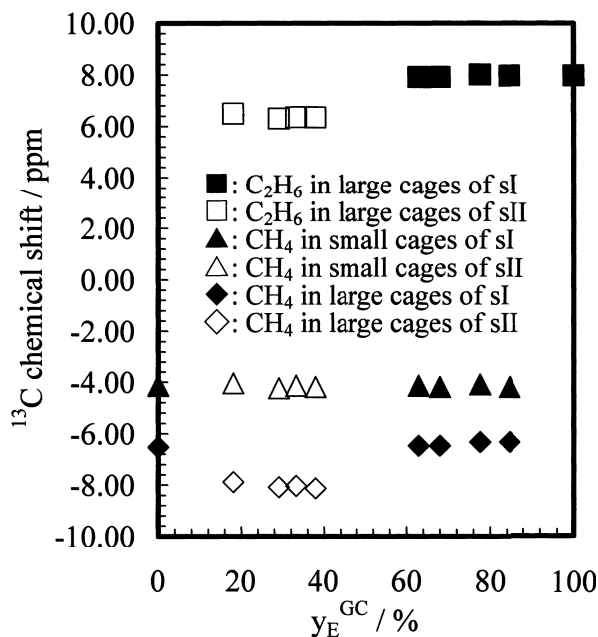


Fig. 2 Changes in  $^{13}\text{C}$  Chemical Shifts in  $\text{CH}_4$ - $\text{C}_2\text{H}_6$  Hydrates with Dissociated  $\text{C}_2\text{H}_6$  Concentrations Measured by Gas Chromatography ( $y_E^{\text{GC}}$ )

$$y_E^{\text{NMR}} = \frac{I_E}{I_M + I_E} \times 100 \quad (1)$$

$I_M$  is the sum of the two integrated peak intensities of  $\text{CH}_4$ , and  $I_E$  is the half value of the integrated peak intensities of  $\text{C}_2\text{H}_6$ .  $^{13}\text{C}$  single-pulse NMR spectra of two samples (b) (**sII**,  $y_E^{\text{GC}} = 18\%$ ) and (d) (**sI**,  $y_E^{\text{GC}} = 63\%$ ) are shown in Fig. 3. The  $\text{C}_2\text{H}_6$  concentrations were calculated as 19% for (b) and 63% for (d) from the NMR spectra. Thus,  $\text{C}_2\text{H}_6$  concentrations determined by the  $^{13}\text{C}$  single-pulse NMR method agreed well with those estimated by gas chromatography ( $y_E^{\text{GC}}$ ). However, sufficiently high quality spectra were difficult to obtain by the  $^{13}\text{C}$  single-pulse method for samples with low concentrations of guest molecules. As shown in Fig. 1, high quality spectra could be obtained by the CP-MAS method for such samples. However, the CP efficiency depends on the type of molecule observed and measurement conditions. Therefore,  $y_E^{\text{NMR}}$  evaluated by Eq. (1) from the CP-MAS  $^{13}\text{C}$  NMR data would not correspond to the real concentration if the CP efficiency for  $\text{CH}_4$  was different from that for  $\text{C}_2\text{H}_6$ . Figure 4 compares the  $\text{C}_2\text{H}_6$  concentrations estimated from CP-MAS  $^{13}\text{C}$  NMR spectra ( $y_E^{\text{NMR}}$ ) with those estimated by gas chromatography ( $y_E^{\text{GC}}$ ), and shows a good correlation (slope = 1.0055, correlation coefficient = 0.9988), implying that the CP efficiency for  $\text{CH}_4$  is approximately the same as that for  $\text{C}_2\text{H}_6$  in these hydrate structures. Although we did not study the difference in CP efficiency between  $\text{CH}_4$  and  $\text{C}_2\text{H}_6$  in detail, the results shown in Figs. 3 and 4 indicate

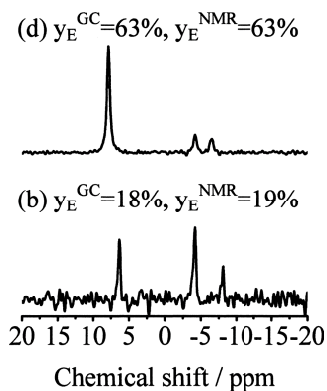
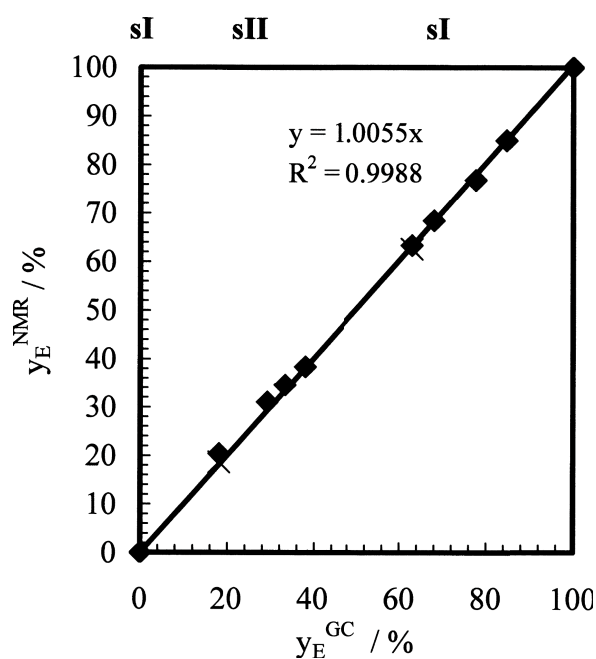


Fig. 3  $^{13}\text{C}$  Single-pulse NMR Spectra of Mixed  $\text{CH}_4\text{-C}_2\text{H}_6$  Hydrates at 163 K

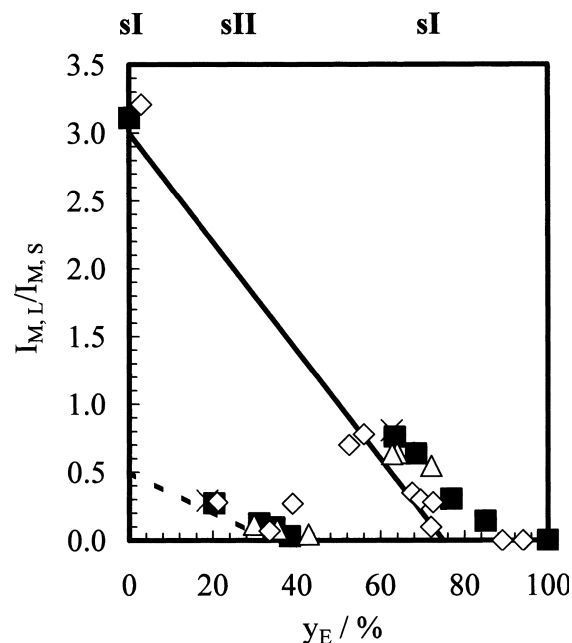


◆: CP-MAS  $^{13}\text{C}$  NMR method, ×:  $^{13}\text{C}$  single-pulse NMR method.

Fig. 4 Relationship between Encaged  $\text{C}_2\text{H}_6$  Concentrations Estimated by  $^{13}\text{C}$  NMR Spectra ( $y_E^{\text{NMR}}$ ) and Dissociated  $\text{C}_2\text{H}_6$  Concentrations Measured by Gas Chromatography ( $y_E^{\text{GC}}$ )

that the compositions of  $\text{CH}_4$  and  $\text{C}_2\text{H}_6$  in the mixed gas hydrates can be directly determined from the CP-MAS  $^{13}\text{C}$  NMR data. In contrast, studies using Raman spectroscopy determined the gas composition of the hydrate phase by gas chromatography. Consequently, CP-MAS  $^{13}\text{C}$  NMR spectroscopy is much more convenient for the determination of hydrate structure and gas composition in the  $\text{CH}_4\text{-C}_2\text{H}_6$  hydrates compared with Raman spectroscopy. Therefore, the  $\text{C}_2\text{H}_6$  concentration evaluated by the CP-MAS  $^{13}\text{C}$  NMR data will be simply expressed as  $y_E$  in the following discussion.

Figure 1 shows that both  $\text{C}_2\text{H}_6$  and  $\text{CH}_4$  molecules



■: CP-MAS  $^{13}\text{C}$  NMR value, ×:  $^{13}\text{C}$  single-pulse NMR value, △: Raman value<sup>4)</sup>, ◇: Raman value<sup>8)</sup>.  
Solid line: full occupancy in sI, Dotted line: full occupancy in sII.

Fig. 5 Changes in the Relative Integrated Signal Intensities Ratio ( $I_{M,L}/I_{M,S}$ ) with  $\text{C}_2\text{H}_6$  Concentration in the Hydrate Phase ( $y_E$ )

in the different cages of the mixed gas hydrates can be distinguished by the  $^{13}\text{C}$  NMR technique. Therefore,  $I_M$  in Eq. (1) can be divided into two peak intensities  $I_{M,S}$  and  $I_{M,L}$ , which are the intensities of  $\text{CH}_4$  in small and large cages, respectively. The ratio of  $I_{M,L}/I_{M,S}$  may reflect the structures of the mixed gas hydrates. For pure  $\text{CH}_4$  hydrate with the sI structure,  $I_{M,L}/I_{M,S}$  should be 3 if all cages are fully occupied by  $\text{CH}_4$ . For pure  $\text{CH}_4$  hydrate with the sII structure,  $I_{M,L}/I_{M,S}$  should be 0.5. If all small cages are occupied by  $\text{CH}_4$  and all large cages by  $\text{CH}_4$  or  $\text{C}_2\text{H}_6$ , the changes in  $I_{M,L}/I_{M,S}$  with  $y_E$  can be expressed by  $(I_{M,L}/I_{M,S}) = 3 - 4y_E$  for sI and  $(I_{M,L}/I_{M,S}) = 0.5 - 1.5y_E$  for sII. The changes in  $I_{M,L}/I_{M,S}$  against  $y_E$  are shown in Fig. 5, where the solid line and the dotted line correspond to full occupancy in the sI and sII structures, respectively. The  $I_{M,L}/I_{M,S}$  values estimated by the CP-MAS  $^{13}\text{C}$  NMR technique for the samples with  $20 \leq y_E \leq 38\%$  decreased with  $y_E$  along the dotted line for sII, and the  $I_{M,L}/I_{M,S}$  values for the samples with  $63 \leq y_E \leq 85\%$  decreased with  $y_E$  along the solid line for sI. The  $I_{M,L}/I_{M,S}$  values estimated by the  $^{13}\text{C}$  single-pulse NMR technique for the same samples were in good agreement. As shown in Fig. 5, the  $I_{M,L}/I_{M,S}$  values obtained in the present study were greater than those assuming full occupancy for both structures, similar to the Raman spectroscopic findings reported previously<sup>4)</sup>. Although a previous study showed almost full occupancy for the samples in this mixed gas system by Raman spectroscopy<sup>8)</sup>, the present

results indicate the presence of some vacant sites in the hydrates.

The present study attempted to estimate the cage occupancies of mixed gas hydrates from the CP-MAS  $^{13}\text{C}$  NMR data using the statistical thermodynamic model<sup>10</sup>. This model has been already applied to estimation of the cage occupancy by the  $^{13}\text{C}$  NMR and Raman techniques<sup>4,6</sup>. The values of  $\theta_S/\theta_L$  in the  $\text{CH}_4\text{-C}_2\text{H}_6$  system are given by Eq. (2) for **sI** and Eq. (3) for **sII**, where  $\theta_S$  and  $\theta_L$  represent the cage occupancies of the small cage and the large cage, respectively.

$$\frac{\theta_S}{\theta_L} = \frac{3I_{M,S}}{I_{M,L} + I_{E,L}}$$

$$\frac{\theta_S}{\theta_L} = \frac{I_{M,S}}{2(I_{M,L} + I_{E,L})} \quad (3)$$

Furthermore,  $\theta_{M,S}$  (small cage occupancy by  $\text{CH}_4$ ),  $\theta_{M,L}$  (large cage occupancy by  $\text{CH}_4$ ), and  $\theta_{E,L}$  (large cage occupancy by  $\text{C}_2\text{H}_6$ ) are given by Eq. (4) for **sI** and Eq.(5) for **sII**, respectively<sup>6,10</sup>.

$$\text{sI} : -\Delta\mu_w^\circ(\text{I}) = \frac{RT}{46} \left[ 6 \ln(1 - \theta_{M,L} - \theta_{E,L}) + 2 \ln(1 - \theta_{M,S}) \right] \quad (4)$$

$$\text{sII} : -\Delta\mu_w^\circ(\text{II}) = \frac{RT}{136} \left[ 8 \ln(1 - \theta_{M,L} - \theta_{E,L}) + 16 \ln(1 - \theta_{M,S}) \right] \quad (5)$$

$\Delta\mu_w^\circ(\text{I})$  and  $\Delta\mu_w^\circ(\text{II})$  are the differences in chemical potentials between ice and the hypothetical empty hydrate lattices of **sI** and **sII**, respectively. The values of  $\Delta\mu_w^\circ(\text{I})$  and  $\Delta\mu_w^\circ(\text{II})$  used here were 1297 J/mol for **sI** and 937 J/mol for **sII**, respectively<sup>15</sup>.  $R$  and  $T$  are the gas constant and temperature for hydrate formation, respectively.

The values for  $\theta_{M,S}$ ,  $\theta_{M,L}$ , and  $\theta_{E,L}$  in **sI** were calculated by Eqs. (2) and (4), and those in **sII** by Eqs. (3) and (5). In both structures, small cage occupancy ( $\theta_S$ ) corresponds to  $\theta_{M,S}$ , because the small cages can encage only  $\text{CH}_4$ . Large cage occupancy ( $\theta_L$ ) is the sum of  $\theta_{M,L}$  and  $\theta_{E,L}$ , since the large cages allow inclusion of both guest molecules. The ratio of  $\theta_{E,L}/\theta_{M,L}$  corresponds to  $I_{E,L}/I_{M,L}$ . The changes in  $\theta_S$  and  $\theta_L$  with  $y_E$  are shown in **Fig. 6**. For pure  $\text{CH}_4$  hydrate, the cage occupancies were estimated as  $\theta_S = 0.94$  and  $\theta_L = 0.97$ , which are almost consistent with those reported for artificial pure  $\text{CH}_4$  hydrate ( $\theta_S = 0.89$  and  $\theta_L = 0.97$ )<sup>6</sup>. The present results show that more than 97% of large cages in both **sI** and **sII** are occupied by  $\text{CH}_4$  and  $\text{C}_2\text{H}_6$ . However,  $\theta_S$  decreases with increasing  $y_E$  ( $\theta_S = 0.82$  at  $y_E = 20\%$  and  $\theta_S = 0.74$  at  $y_E = 38\%$  in the region of **sII**, and  $\theta_S = 0.77$  at  $y_E = 63\%$  and  $\theta_S = 0.45$  at  $y_E = 85\%$  in the region of **sI**). Accordingly, the higher values of  $I_{M,L}/I_{M,S}$  in **Fig. 5** reflects the decrease in  $\theta_S$  with increase in  $y_E$ .

The changes in the guest molecule distribution in the

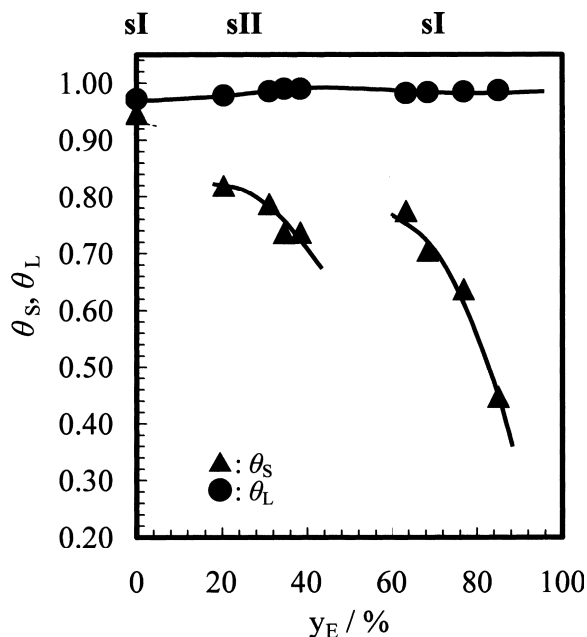


Fig. 6 Changes in the Occupancies of Small Cages ( $\theta_S$ ) and Large Cages ( $\theta_L$ ) with  $\text{C}_2\text{H}_6$  Concentration in the Hydrate Phase ( $y_E$ )

large cages with increasing  $\text{C}_2\text{H}_6$  concentration are shown in **Fig. 7**. The  $\theta_{E,L}$  in the region of **sII**,  $20 \leq y_E \leq 38\%$ , increases with increasing  $y_E$ , whereas the  $\theta_{M,L}$  decreases in this region. The values of  $\theta_{M,L}$  and  $\theta_{E,L}$  for the sample with  $y_E = 38\%$  were 0.05 and 0.94, respectively, indicating that the large cages of **sII** in this sample were almost completely occupied by  $\text{C}_2\text{H}_6$ . At  $y_E = 63\%$ , the structure was **sI** and  $\theta_{M,L}$  was 0.20. Then,  $\theta_{M,L}$  decreases toward zero with increasing  $\text{C}_2\text{H}_6$  concentration. Thus, the large cages in both **sI** and **sII** were preferentially occupied by  $\text{C}_2\text{H}_6$ . As can be seen from **Fig. 6**,  $\theta_S$  rapidly decreased with increasing  $y_E$  in the region of **sII**. The pure  $\text{C}_2\text{H}_6$  hydrate has the **sI** structure with  $\theta_S = 0$ , indicating that **sII** at the low level of  $\theta_S$  is more unstable than **sI**. Therefore, excessive decrease in  $\theta_S$  in **sII** might induce structural change from **sII** to **sI** at higher concentrations of  $\text{C}_2\text{H}_6$ .

#### 4. Conclusions

The present study obtained high quality CP-MAS  $^{13}\text{C}$  NMR spectra of mixed  $\text{CH}_4\text{-C}_2\text{H}_6$  gas hydrates at 163 K without using  $^{13}\text{C}$ -enriched gases. The changes in the NMR chemical shifts clearly corresponded to the structural changes in the hydrate structure (**sI** for pure  $\text{CH}_4$  hydrate, **sII** in the range of  $20 \leq y_E \leq 38\%$ , and **sI** in the range  $63\% \leq y_E$ ), and agreed with the findings of other techniques such as the XRD method and Raman spectroscopy. The present study also clarified that the gas compositions estimated by the CP-MAS  $^{13}\text{C}$  NMR spectra agreed well with the corresponding dissociated gases measured by gas chromatography and compo-

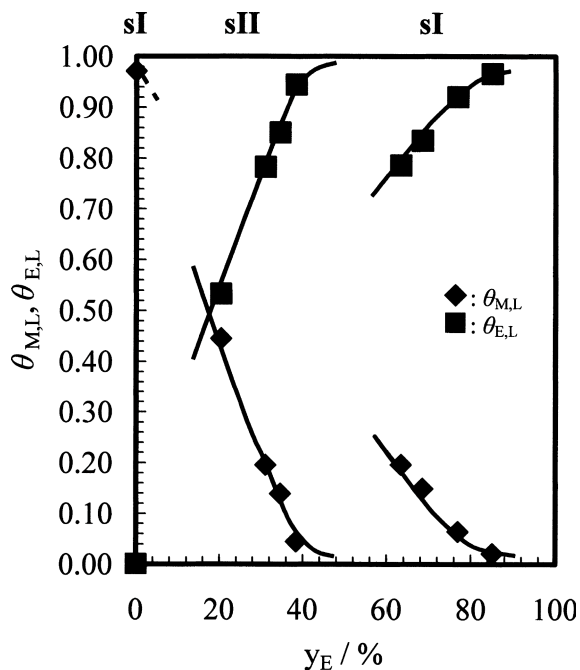


Fig. 7 Changes in the Guest Molecule Distribution in the Large Cages with  $C_2H_6$  Concentration in the Hydrate Phase ( $y_E$ )

sitions estimated by the  $^{13}C$  single-pulse NMR spectra, indicating that the gas composition in the mixed gas hydrates can be directly estimated from the CP-MAS  $^{13}C$  NMR spectra. The occupancies of small cages and large cages were evaluated from the  $^{13}C$  NMR data based on the statistical thermodynamic model, which showed that the occupancies of small cages decreased with increasing  $C_2H_6$  concentration in both sI and sII structures, whereas the occupancy of large cages was unchanged through a wide range of  $C_2H_6$  concentrations at almost the full occupancy level.

#### Acknowledgment

We thank Dr. T. Uchida (Hokkaido University) for fruitful discussions.

#### References

- 1) Sloan Jr., E. D., "Clathrate Hydrates of Natural Gases, 2nd ed," Marcel Dekker Inc., New York (1998), p. 1-64.
- 2) Davidson, D. W., Garg, S. K., Gough, S. R., Handa, Y. P., Ratcliffe, C. I., Ripmeester, J. A., Tse, J. S., Lawson, W. F., *Geochim. Cosmochim. Acta.*, **50**, 619 (1986).
- 3) Ripmeester, J. A., Tse, J. S., Ratcliffe, C. I., Powell, B. M., *Nature*, **325**, 135 (1987).
- 4) Subramanian, S., Kini, R. A., Dec, S. F., Sloan Jr., E. D., *Chem. Eng. Sci.*, **55**, 1981 (2000).
- 5) Takeya, S., Kamata, Y., Uchida, T., Nagao, J., Ebinuma, T., Narita, H., Hori, A., Hondoh, T., *Can. J. Phys.*, **81**, 479 (2003).
- 6) Ripmeester, J. A., Ratcliffe, C. I., *J. Phys. Chem.*, **92**, 337 (1988).
- 7) Takeya, S., Kida, M., Minami, H., Sakagami, H., Hachikubo, A., Takahashi, N., Shoji, H., Soloviev, V., Wallmann, K., Biebow, N., Obzhairov, A., Salomatin, A., Poort, J., *Chem. Eng. Sci.*, **61**, 2670 (2006).
- 8) Uchida, T., Takeya, S., Kamata, Y., Ikeda, Y. I., Nagao, J., Ebinuma, T., Narita, H., Zatsepina, O., Buffett, B. A., *J. Phys. Chem. B*, **106**, 12426 (2002).
- 9) Sum, A. K., Burruss, R. C., Sloan Jr., E. D., *J. Phys. Chem. B*, **101**, 7371 (1997).
- 10) van der Waals, J. H., Platteeuw, J. C., *Adv. Chem. Phys.*, **2**, 1 (1959).
- 11) Lee, J. W., Lu, H., Moudrakovski, I. L., Ratcliffe, C. I., Ripmeester, J. A., *Angew. Chem. Int. Ed.*, **45**, 2456 (2006).
- 12) Pines, A., Gibby, M. G., Waugh, J. S., *J. Chem. Phys.*, **59**, 569 (1973).
- 13) Schaefer, J., Stejskal, E. O., *J. Am. Chem. Soc.*, **98**, 1031 (1976).
- 14) Hayashi, S., Hayamizu, K., *Bull. Chem. Soc. Jpn.*, **64**, 685 (1991).
- 15) Dharmawardhana, P. B., Parrish, W. R., Sloan, E. D., *Ind. Eng. Chem., Fundam.*, **19**, 410 (1980).

## 要 旨

CP-MAS  $^{13}\text{C}$  NMR 法によるメタン-エタン混合ガスハイドレートのガス組成およびケージ占有率評価

木田 真人<sup>†1)</sup>, 坂上 寛敏<sup>†1)</sup>, 高橋 信夫<sup>†1)</sup>, 八久保 晶弘<sup>†2)</sup>, 庄子 仁<sup>†2)</sup>,  
鎌田 慈<sup>†3),†5)</sup>, 海老沼 孝郎<sup>†3)</sup>, 成田 英夫<sup>†3)</sup>, 竹谷 敏<sup>†4)</sup>

<sup>†1)</sup> 北見工業大学機能材料工学科, 090-8507 北海道北見市公園町165

<sup>†2)</sup> 北見工業大学未利用エネルギー研究センター, 090-8507 北海道北見市公園町165

<sup>†3)</sup> (独)産業技術総合研究所 メタンハイドレート研究ラボ, 062-8517 札幌市豊平区月寒東2-17

<sup>†4)</sup> (独)産業技術総合研究所 計測フロンティア研究部門, 305-8565 茨城県つくば市東1-1-1中央第5

<sup>†5)</sup> (現在)(財)鉄道総合研究所 防災技術研究部, 185-8540 東京都国分寺市光町2-8-38

本研究では, メタン-エタン混合ガスハイドレートの CP-MAS  $^{13}\text{C}$  NMR 測定を行った。得られたメタンとエタンの  $^{13}\text{C}$  ケミカルシフト値はハイドレート構造の変化に対応した。包接ガス組成は得られた  $^{13}\text{C}$  NMR シグナルの積分強度比から見積もられ, ガスクロマトグラフィーによって見積もられた分解ガス組成と良い一致を示した。このことから, 混合ガスハイドレート中のガス組成は  $^{13}\text{C}$  NMR スペクトルによって直接算出可能

である。得られた  $^{13}\text{C}$  NMR スペクトルおよび統計熱力学モデルに基づき, ハイドレートの小ケージおよび大ケージ占有率を算出した。その結果, 大ケージはガス組成によらずほぼゲスト分子によって占有されているのに対して, 小ケージ占有率はエタン組成増加に伴い減少することが示された。さらに, 大ケージはメタン分子よりエタン分子によって優先的に占有されることが示唆された。